Inorg. Chem. **2007**, *46*, 4458–4468

Inorganic Chemistry
Article

Magnetic Interactions in Cu^{II}–Ln^{III} Cyclic Tetranuclear Complexes: Is It Possible to Explain the Occurrence of SMM Behavior in Cu^{II}–Tb^{III} and Cu^{II}–Dy^{III} Complexes?

Takefumi Hamamatsu,[†] Kazuya Yabe,[†] Masaaki Towatari,[†] Shutaro Osa,[†] Naohide Matsumoto,*[,†] Nazzareno Re,[‡] Andrzej Pochaba,[§] Jerzy Mrozinski,[§] Jean-Louis Gallani,*[,∥] Alessandro Barla,[∥] Paolo Imperia,[⊥] Carley Paulsen,[¶] and Jean-Paul Kappler[∥]

Department of Chemistry, Faculty of Science, Kumamoto University, Kurokami 2-39-1, Kumamoto 860-8555, Japan, Facolta di Farmacia, Università degli Studi "G. D'Annunzio", I-66100 Chieti, Italy, Faculty of Chemistry, University of Wroclaw, 14, F. Joliot-Curie, 50-383 Wroclaw, Poland, IPCMS, UMR7504, 23 rue du Loess, BP 43, 67034 Strasbourg Cedex 2, France, BESSY, Albert-Einstein-Str. 15, 12489 Berlin, Germany, and CRTBT-CNRS, BP166, 38042 Grenoble Cedex 9, France

Received November 26, 2006

An extensive series of tetranuclear $Cu^{II}_2Ln^{III}_2$ complexes $[Cu^{II}LLn^{III}(hfac)_2]_2$ (with Ln^{III} being all lanthanide(III) ions except for the radioactive Pm^{III}) has been prepared in order to investigate the nature of the Cu^{II}–Ln^{III} magnetic interactions and to try to answer the following question: What makes the $Cu^{II}_2Tb^{III}_2$ and $Cu^{II}_2Dy^{III}_2$ complexes single molecule magnets while the other complexes are not? All the complexes within this series possess a similar cyclic tetranuclear structure, in which the Cu^{II} and Ln^{III} ions are arrayed alternately via bridges of ligand complex ($Cu^{II}L$). Regular SQUID magnetometry measurements have been performed on the series. The temperature-dependent magnetic susceptibilities from 2 to 300 K and the field-dependent magnetizations from 0 to 5 T at 2 K have been measured for the $Cu^{II}_2Ln^{III}_2$ and $Ni^{II}_2Ln^{III}_2$ complexes, with the $Ni^{II}_2Ln^{III}_2$ complex containing diamagnetic Ni^{II} ions being used as a reference for the evaluation of the Cu^{II}–Ln^{III} magnetic interactions. These measurements have revealed that the interactions between Cu^{II} and Ln^{III} ions are very weakly antiferromagnetic if Ln = Ce, Nd, Sm, Yb, ferromagnetic if Ln = Gd, Tb, Dy, Ho, Er, Tm, and negligible if Ln = La, Eu, Pr, Lu. With the same goal of better understanding the evolution of the intramolecular magnetic interactions, X-ray magnetic circular dichroism (XMCD) has also been measured on $Cu^{II}_2Tb^{III}_2$, $Cu^{II}_2Dy^{III}_2$, and $Ni^{II}_2Tb^{III}_2$ complexes, either at the *L*- and *M*-edges of the metal ions or at the *K*-edge of the N and O atoms. Last, the $Cu^{II}_2Tb^{III}_2$ complex exhibiting SMM behavior has received a closer examination of its low temperature magnetic properties down to 0.1 K. These particular measurements have revealed the unusual very slow setting-up of a 3D order below 0.6 K.

Introduction

Since the first discovery in 1993 that the metallic cluster called Mn_{12} acetate, or Mn_{12}, could behave as a magnet, i.e., retain some magnetization at the molecular level, so-called single molecule magnets or SMMs have attracted special attention.[1] On the basis of the theoretical and experimental results reported so far, it is now well-established that the required conditions for the observation of such a particular behavior are a high spin ground state and a large easy-axis type magnetic anisotropy. This then results in a magnetic bistable molecule with a significant energy barrier to thermally activated magnetization relaxation.[2] Since the conditions to be an SMM, high spin ground state and magnetic anisotropy, are not easily achieved and the blocking temperatures T_B of the SMM reported so far are still well below liquid helium temperature, alternative and new molecular designs are much sought after. Ishikawa's group

* To whom correspondence should be addressed. E-mail: naohide@aster.sci.kumamoto-u.ac.jp (N.M.), gallani@ipcms.u-strasbg.fr (J.-L.G.).
[†] Kumamoto University.
[‡] Università degli Studi "G. D'Annunzio".
[§] University of Wroclaw.
[∥] IPCMS.
[⊥] BESSY.
[¶] CRTBT-CNRS.

10.1021/ic062252s CCC: $37.00
Published on Web 04/26/2007

reported that Tb^{III}, Dy^{III}, and Ho^{III} phtalocyanines exibit SMM behavior showing that even a mononuclear 4f molecule can behave as an SMM.[3] On the basis of the conditions of high-spin ground state and magnetic anisotropy required for SMMs, we designed a cyclic tetranuclear $[Cu^{II}_2Tb^{III}_2]$ complex, $[Cu^{II}LTb^{III}(hfac)_2]_2$, and reported the first 3d−4f SMM published in the literature, where H_3L = 1-(2-hydroxybenzamido)-2-(2-hydroxy-3-methoxybenzylideneamino)ethylene, and Hhfac = hexafluoroacetylacetone.[4] There are several advantages in favor of the 3d−4f approach for building up molecules with SMM behavior: (1) the high-spin ground state can be obtained by the ferromagnetic coupling between 3d and 4f ions, and (2) the molecular magnetic anisotropy is derived from the 4f-component such as the Tb^{III} ion. In recent years, the molecular design of SMMs and single-chain magnets (SCMs) containing f-block elements has attracted much attention.[5−11] Christou's group[5] and Pecoraro's group[6] synthesized $Mn^{III}-Dy^{III}$ clusters and reported their magnetic properties. $[Mn^{III}_{11}Dy^{III}_4]$ and $[Mn^{III}_2Dy^{III}_2]$ clusters reported by Christou's group[5] are confirmed to exhibit temperature and sweep rate dependent hysteresis loops, a trademark of all SMMs. Furthermore, several reports on d−f clusters, $[Cu^{II}Tb^{III}]$ binuclear and $[Cu^{II}_2Tb^{III}_2]$ tetranuclear complexes,[7] a $[Cu^{II}Tb^{III}_4]$ pentanuclear complex,[8] $[Cu^{II}_6Dy^{III}_3]$ nonanuclear complexes,[9] a $[Fe^{III}Dy^{III}]$ binuclear complex,[10a] and a $[Cu^{II}Dy^{III}_2]$ trinuclear complex[10b] have appeared in the most recent literature. These studies demonstrate that the d−f cluster approach is a very promising pathway to SMMs.

At present, only the f and d−f complexes involving Tb^{III}, Dy^{III}, and Ho^{III} ions have been reported to show SMM behavior. Among the 15 lanthanide ions, 12 exhibit magnetic anisotropy due to the first-order orbital angular momentum while La^{III} and Lu^{III} are diamagnetic and Gd^{III} is spin-only. (The ground state electronic properties of the Ln^{III} ions are given in a table of Supporting Information.) Since the d−f complexes with the 12 Ln^{III} ions of $[Cu^{II}LLn^{III}(hfac)_2]_2$ might retain the magnetic anisotropy, the possibility of getting SMM behavior with some of these complexes deserved to be investigated. In this study, we therefore prepared a whole series of the $Cu^{II}_2Ln^{III}_2$ complexes with all lanthanide ions, except for the radioactive Pm^{III}. The goal was to investigate the nature of the $Cu^{II}-Ln^{III}$ magnetic interactions and to try to answer the following question: Which lanthanide should be associated to Cu^{II} in $[Cu^{II}LLn^{III}(hfac)_2]_2$ for synthesizing single molecule magnets? Some of the complexes reported in this paper (Ln = Eu, Gd, Tb, and Dy) have already been studied with the results published elsewhere,[12] and preliminary results on the SMM behavior of the $Cu^{II}_2Tb^{III}_2$ and $Cu^{II}_2Dy^{III}_2$ complexes have also been reported.[4] We now present a much more detailed investigation, which results from very specialized techniques, namely very low temperature SQUID magnetometry and X-ray magnetic circular dichroism (XMCD). As will be shown hereafter, the SMM behavior of the $Cu^{II}_2Tb^{III}_2$ complex is now confirmed thanks to these complementary SQUID measurements, which have also revealed the unusual very slow setting-up of 3D order below 0.6 K. The XMCD measurements provide some insight on the magnetic moments on the metallic ions and on the polarization of oxygen atoms.

Results and Discussion

Synthesis and Characterization of Cyclic Tetranuclear $Cu^{II}_2Ln^{III}_2$ and $Ni^{II}_2Ln^{III}_2$ Complexes $[M^{II}LLn^{III}(hfac)_2]_2$. A complete series of tetranuclear $Cu^{II}_2Ln^{III}_2$ complexes $[Cu^{II}LLn^{III}(hfac)_2]_2$ has been prepared according to the method reported previously, where Ln^{III} denotes all lanthanide(III) ions except for the radioactive Pm^{III}, H_3L denotes an unsymmetrical tetradentate ligand, 1-(2-hydroxybenzamido)-2-(2-hydroxy-3-methoxybenzylideneamino)ethylene, and Hhfac denotes hexafluoroacetylacetone.[12] As is shown in Scheme 1, the simple mixing of methanolic solutions of $K[Cu^{II}L]$[13] and $Ln^{III}(hfac)_3(H_2O)_2$ in a 1:1 mole ratio gave a tetranuclear complex, $[Cu^{II}LLn^{III}(hfac)_2]_2$, in high yields (ca. 90%), where one $hfac^-$ ligand per Ln^{III} ion is eliminated during the reaction to give an electrically neutral species $[Cu^{II}LLn^{III}(hfac)_2]_2$. The reference complexes containing the

(1) (a) Sessoli, R.; Gatteschi, D.; Caneschi, A.; Novak, M. A. *Nature* **1993**, *365*, 141−143. (b) Gatteschi, D.; Caneschi, A.; Pardi, L.; Sessoli, R. *Science* **1994**, *265*, 1054−1058. (c) Sessoli, R.; Tsai, H. L.; Schake, A. R.; Wang, S.; Vincent, J. B.; Folting, K.; Gatteschi, D.; Christou, G.; Hendrickson, D. N. *J. Am. Chem. Soc.* **1993**, *115*, 1804−1816. (d) Thomas, L.; Lionti, F.; Ballou, R.; Gatteschi, D.; Sessoli, R.; Barbara, B. *Nature* **1996**, *383*, 145−147. (e) Cadiou, C.; Murrie, M.; Paulsen, C.; Villar, V.; Wernsdorfer, W.; Winpenny, W. E. P. *Chem. Commun*. **2001**, 2666−2667. (f) Shores, M. P.; Sokol, J. J.; Long, J. R. *J. Am. Chem. Soc.* **2002**, *124*, 2279−2292. (g) Boskovic, C.; Brechin, E. K.; Streib, W. E.; Folting, K.; Bollinger, J. C.; Hendrickson, D. N.; Christou, G. *J. Am. Chem. Soc.* **2002**, *124*, 3725−3736. (h) Ritter, S. *Chem. Eng. News* **2004**, *82*, 29−32.

(2) Gatteschi, D.; Sessoli, R. *Angew. Chem., Int. Ed.* **2003**, *42*, 268−297 and references therein.

(3) (a) Ishikawa, N.; Sugita, M.; Wernsdorfer, W. *J. Am. Chem. Soc.* **2005**, *127*, 3650−3651. (b) Ishikawa, N.; Sugita, M.; Tanaka, N.; Ishikawa, T.; Koshihara, S.; Kaizu, Y. *Inorg. Chem.* **2004**, *43*, 5498−5500.

(4) Osa, S.; Kido, T.; Matsumoto, N.; Re, N. Pochaba, A.; Mrozinski, J. *J. Am. Chem. Soc.* **2004**, *126*, 420−421.

(5) (a) Mishra, A.; Wernsdorfer, W.; Abboud, K. A.; Christou, G. *J. Am. Chem. Soc.* **2004**, *126*, 15648−15649. (b) Mishra, A.; Wernsdorfer, W.; Parsons, S.; Christou, G.; Brechin, F. K. *Chem. Commun.* **2005**, 2086−2088.

(6) Zaleski, C. M.; Depperman, E. C.; Kampf, J. W.; Kirk, M. L.; Pecoraro, V. *Angew. Chem., Int. Ed.* **2004**, *43*, 3912−3914.

(7) (a) Costes, J.-P.; Dahan, F.; Wernsdorfer, W. *Inorg. Chem*. **2006**, *45*, 5−7. (b) He, F.; Tong, M.-L.; Chen, X.-M. *Inorg. Chem.* **2005**, *44*, 8285−8292. (c) Costes, J.-P.; Auchel, M.; Dahan, F.; Peyrou, V.; Shova, S.; Wernsdorfer, W. *Inorg. Chem*. **2006**, *45*, 1924−1934.

(8) (a) Ueki, S.; Sahlan, M.; Ishida, T.; Nogami, T. *Synth. Met.* **2005**, *154*, 217. (b) Mori, F.; Ishida, T.; Nogami, T. *Polyhedron* **2005**, *24*, 2588. (c) Mori, F.; Nyui, T.; Ishida, T.; Nogami, T.; Choi, K.-Y.; Nojiri, H. *J. Am. Chem. Soc.* **2006**, *128*, 1440.

(9) Aronica, C.; Pilet, G.; Chastanet, G.; Wernsdorfer, W.; Jacquot, J.-P.; Luneau, D. *Angew. Chem., Int. Ed.* **2006**, *45*, 4659−4662.

(10) (a) Ferbinteanu, M.; Kajiwara, T.; Choi, K.-Y.; Nojiri, H.; Nakamoto, A.; Kojima, N.; Cimpoesu, F.; Fujimura, Y.; Takaishi, S.; Yamashita, M. *J. Am. Chem. Soc.* **2006**, *128*, 9008−9009. (b) Pointillart, F.; Bernot, K.; Sessoli, R.; Gatteschi, D. *Chem. Eur. J.* **2007**, *13*, 1602−1609.

(11) (a) Tang, J.; Hewitt, I.; Madhu, N. T.; Chastanet, G.; Wernsdorfer, W.; Ansen, C. E.; Benelli, C.; Sessoli, R.; Powell, A. K. *Angew. Chem., Int. Ed.* **2006**, *45*, 1729−1733. (b) Bernot, K.; Bogani, L.; Caneschi, A.; Gatteschi, D.; Sessoli, R. *J. Am. Chem. Soc.* **2006**, *128*, 7947−7956. (c) Bogani, L.; Sangregorio, C.; Sessoli, R.; Gatteschi, D. *Angew. Chem., Int. Ed.* **2005**, *44*, 5817−5821.

(12) (a) Kido, T.; Nagasato, S.; Sunatsuki, Y.; Matsumoto, N. *Chem. Commun.* **2000**, 2113−2114. (b) Kido, T.; Ikuta, Y.; Sunatsuki, Y.; Ogawa, Y.; Matsumoto, N.; Re, N. *Inorg. Chem.* **2003**, *42*, 398−408.

(13) Sunatsuki, Y.; Matsuo, T.; Nakamura, M.; Kai, F.; Matsumoto, N.; Tuchagues, J.-P. *Bull. Chem. Soc. Jpn.* **1998**, *71*, 2611−2619.

Scheme 1. Reaction Scheme from $K[Cu^{II}L]$ (or $K[Ni^{II}L]\cdot 2H_2O$) and $Ln^{III}(hfac)_3(H_2O)_2$ in a 1:1 Mole Ratio to Electrically Neutral Species $[Cu^{II}LLn^{III}(hfac)_2]_2$ (or $[Ni^{II}LLn^{III}(hfac)_2]_2$)

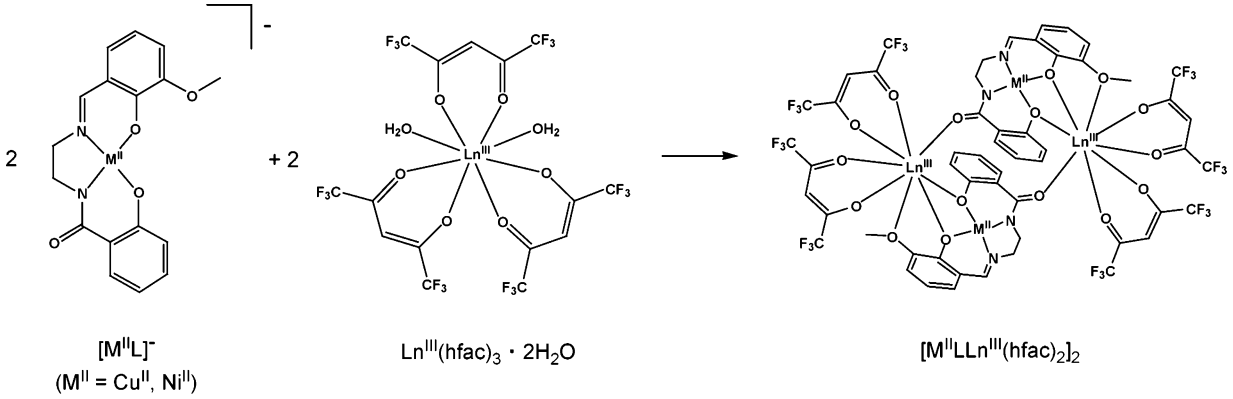

diamagnetic Ni^{II} ion, $[Ni^{II}LLn^{III}(hfac)_2]_2$, were prepared with a method similar to that used for preparing $[Cu^{II}LLn^{III}(hfac)_2]_2$ by mixing $K[Ni^{II}L]\cdot 2H_2O$[13] and $Ln^{III}(hfac)_3(H_2O)_2$. Elemental analytical data for C, H, and N elements of all 28 complexes agree well with their calculated values, and these data are given as Supporting Information. Each infrared spectrum of the tetranuclear complexes $[Cu^{II}LLn^{III}(hfac)_2]_2$ and $[Ni^{II}LLn^{III}(hfac)_2]_2$ exhibits an intense absorption band assignable to the $\nu_{C=O}$ vibration of the amido moiety at 1651−1652 cm^{-1}, whose wavenumber is shifted to a higher value from 1644 cm^{-1} of the component complex $K[Cu^{II}L]$ and from 1625 cm^{-1} of $K[Ni^{II}L]\cdot 2H_2O$.[13]

This shift is related to the weaker coordination of the amido group to the Ln^{III} ion, as compared to the coordination of the amido group to the K^+ ion.[12] Since $Cu^{II}_2Ln^{III}_2$ and $Ni^{II}_2Ln^{III}_2$ complexes are sparingly soluble in water and common organic solvents, recrystallization was not performed. Well-grown crystals were obtained using the diffusion method. The crystalline samples obtained this way were used for all the physical measurements including elemental analyses, infrared spectra, X-ray analyses, and magnetic measurements.

Structural Description of $Cu^{II}_2Ln^{III}_2$ and $Ni^{II}_2Ln^{III}_2$ Complexes. Well-grown crystals of $Cu^{II}_2Ln^{III}_2$ complexes suitable for the single-crystal X-ray diffraction study were obtained using the diffusion method, but those of $Ni^{II}_2Ln^{III}_2$ complexes were not obtained. The powder X-ray diffraction patterns showed that the $Cu^{II}_2Ln^{III}_2$ complexes are isomorphous to each other. The powder X-ray diffraction patterns showed that the $Ni^{II}_2Ln^{III}_2$ complexes are isomorphous to each other but are not isomorphous to the $Cu^{II}_2Ln^{III}_2$ complexes. FAB-MS of the $Ni^{II}_2Ln^{III}_2$ complexes shows a molecular ion peak corresponding to the tetranuclear species $[Ni_2L_2Ln_2(hfac)_3]^+$, indicating that the $Ni^{II}_2Ln^{III}_2$ complex assumes a tetranuclear structure similar to that of the Cu^{II}_2-Ln^{III}_2 complex. The crystal structures of selected $Cu^{II}_2Ln^{III}_2$ complexes with Gd, Tb, and Dy were determined by single-crystal X-ray diffraction analyses and have been reported previously.[12] Their crystallographic data revealed that they are isomorphous to each other. Figure 1 shows a cyclic $Cu^{II}_2Gd^{III}_2$ tetranuclear structure with the atom numbering scheme, in which the cyclic tetranuclear molecule has an inversion center and the Cu^{II} and Gd^{III} ions are arrayed alternately. In the cyclic structure, the Cu^{II} complex functions as an electrically mononegative "bridging ligand-complex" to the two Gd^{III} ions. The two phenoxo (O(2) and O(3)) and the methoxy (O(4)) atoms at one side of the planar Cu^{II} complex coordinate to a Gd^{III} ion as a tridentate ligand with distances of Gd−O(2) = 2.467(3) Å, Gd−O(3) = 2.350(3) Å, Gd−O(4) = 2.542(3) Å, and Cu−Gd = 3.432(1) Å. The amido oxygen atom (O(1)) on the opposite side of the Cu complex coordinates to another Gd^{III} ion as a monodentate ligand with the distance of Gd*−O(1) = 2.275(3) Å and Cu−Gd* = 5.620(3) Å. Including the coordination of the two $hfac^-$ ions as a bidentate chelate ligand (Gd−O = 2.337(4)−2.407(4) Å), the Gd ion has an octacoordinate geometry with the O_8 oxygen atoms. It should be noted that the Gd−O bond distance with the amido oxygen is the shortest among the eight Gd−O coordination bonds. In a cyclic structure, there is no bridging ligand between the two Cu^{II} ions and between the two Gd^{III} ions. The cyclic tetranuclear molecules are separated in the crystal, and the compound can be described as an isolated molecule.

Static Magnetic Properties of $Cu^{II}_2Ln^{III}_2$ Complexes. The magnetic susceptibilities, χ_M's, of all tetranuclear complexes $[Cu^{II}LLn^{III}(hfac)_2]_2$ from the series have been measured under an external applied magnetic field of 1 T in the temperature range 2−300 K. The plots of $\chi_M T$ versus temperature T are shown in Figure 2a,b. It can be seen that, except for those involving the Gd, Tb, and Dy

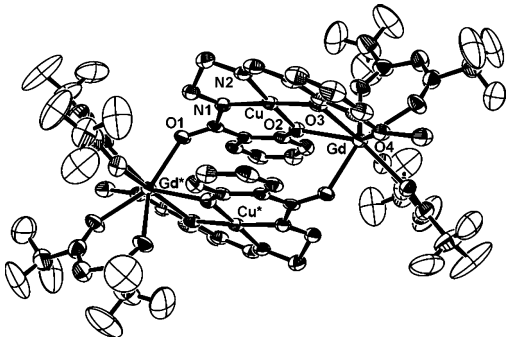

Figure 1. Molecular structure of cyclic tetranuclear complex $[Cu^{II}LGd^{III}(hfac)_2]_2$ with selected atom labeling scheme. The hydrogen atoms are omitted for clarity. The structure is drawn from the data reported previously.[12]

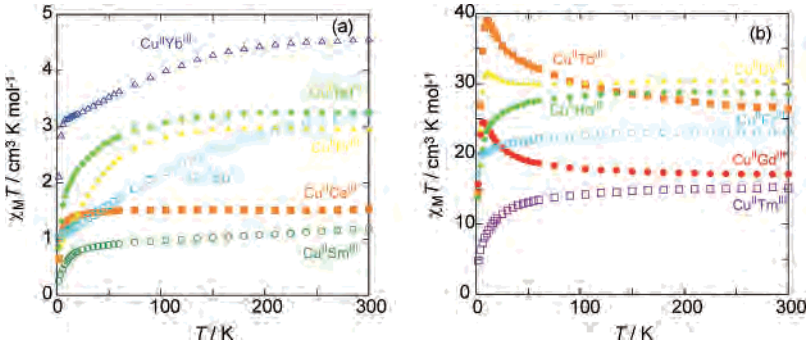

Figure 2. Evolution of $\chi_M T$ vs temperature (T) for the whole series of $Cu^{II}_2Ln^{III}_2$ complexes. (a) Plots for the complexes with Ce, Pr, Nd, Sm, Eu, and Yb. (b) Plots for the complexes with Gd, Tb, Dy, Ho, Er, and Tm.

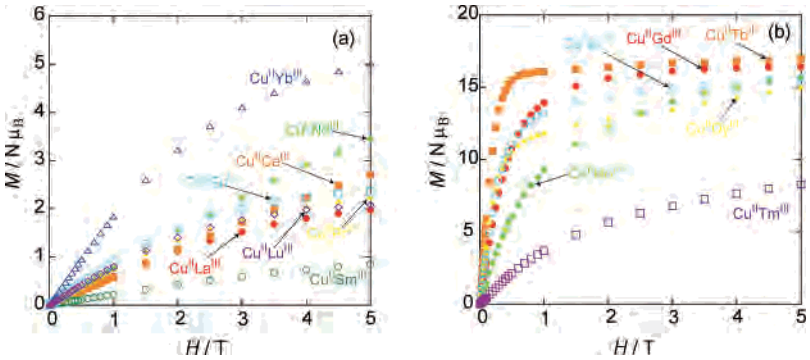

Figure 3. Field dependence of the magnetization M at 2 K as a function of the applied magnetic field H for the whole series of tetranuclear $Cu^{II}_2Ln^{III}_2$ complexes. (a) Plots for the complexes with La, Ce, Pr, Nd, Sm, Eu, Yb, and Lu as being noted as $Cu^{II}Ln^{III}$. (b) Plots for the complexes with Gd, Tb, Dy, Ho, Er, and Tm as being noted as $Cu^{II}Ln^{III}$.

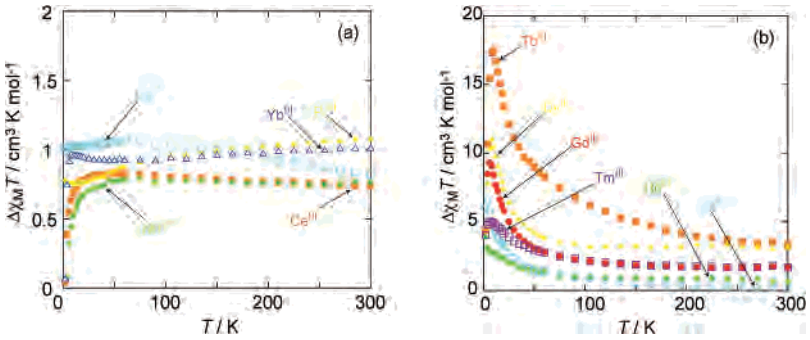

Figure 4. Plots of $\Delta(T) = (\chi_M T)_{Cu2Ln2} - (\chi_M T)_{Ni2Ln2}$ vs temperature T for all tetranuclear $Cu^{II}_2Ln^{III}_2$ complexes. (a) Plots for the complexes with Ce, Pr, Nd, Eu, and Yb as being noted as $Cu^{II}Ln^{III}$. (b) Plots for the complexes with Gd, Tb, Dy, Ho, Er, and Tm as being noted as $Cu^{II}Ln^{III}$.

ions, all complexes showed the decrease of the $\chi_M T$ value on lowering the temperature.

The field-dependent magnetizations were measured at 2 K with an applied magnetic field of 0−5 T. Figure 3a,b shows the magnetization M as a function of the applied field H for all the $Cu^{II}_2Ln^{III}_2$ complexes. The magnetization curves of the complexes with Gd, Tb, and Dy show a rather abrupt increase in weak magnetic fields (in particular the $Cu^{II}_2Tb^{III}_2$ complex) whereas the magnetization of the other complexes does not even saturate (e.g., $Cu^{II}_2Sm^{III}_2$ or $Cu^{II}_2Ce^{III}_2$).

Nature of the Magnetic Interaction between Cu^{II} and Ln^{III} Ions. The nature of the magnetic interactions in the complexes between Cu^{II} and Ln^{III} ions was first investigated by an empirical approach based on a comparison of the magnetic susceptibilities of $Cu^{II}_2Ln^{III}_2$ with those of the isostructural $Ni^{II}_2Ln^{III}_2$ complexes involving the diamagnetic Ni^{II} ion. For these comparisons, we shall make use of the variable Δ defined as $\Delta(T) = (\chi_M T)_{Cu2Ln2} - (\chi_M T)_{Ni2Ln2}$, obtained experimentally. By assuming negligible intramolecular $Ln^{III}-Ln^{III}$ and $Cu^{II}-Cu^{II}$ magnetic interactions due to the lack of magnetic mediators, we can immediately write the equation $\Delta(T) = (\chi_M T)_{Cu2Ln2} - (\chi_M T)_{Ni2Ln2} = 2(\chi_M T)_{Cu} + 2J_{CuLn}(T)$, where $(\chi_M T)_{Cu}$ represents the $\chi_M T$ value imputable to an isolated Cu^{II} ion (Curie constant $(\chi_M T)_{Cu} = 0.375$ $cm^3 \cdot K \cdot mol^{-1}$) and the temperature-dependent contribution $J_{CuLn}(T)$ is related to the nature of the overall exchange interactions between the Cu^{II} and Ln^{III} ions. In particular, a positive or a negative value of this contribution is directly related to a ferro- or antiferromagnetic interaction, respectively. The plots of $\Delta(T)$ versus T for all compounds are given in Figure 4a,b. Since $2J_{CuLn}(T) = \Delta(T) - 2(\chi_M T)_{Cu}$, when the $\Delta(T)$ value is larger than $2(\chi_M T)_{Cu} = 0.75$ $cm^3 \cdot K \cdot mol^{-1}$, $2J_{CuLn}(T)$ is positive, and consequently, the magnetic interactions between Cu^{II} and Ln^{III} ions are

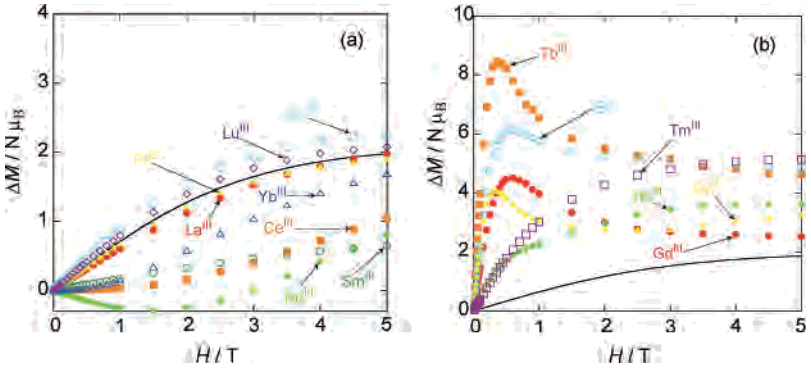

Figure 5. Plots of $\Delta(H) = M_{Cu2Ln2}(H) - M_{Ni2Ln2}(H)$ vs H for the whole series of tetranuclear $Cu^{II}_2Ln^{III}_2$ complexes. Black solid lines are the theoretical magnetization curves (Brillouin functions) of two independent Cu^{II} ions with $S = {}^1/_2$ and $g = 2.00$. (a) Plots for the complexes with La, Ce, Pr, Nd, Sm, Eu, Yb, and Lu. (b) Plots for the complexes with Gd, Tb, Dy, Ho, Er, and Tm.

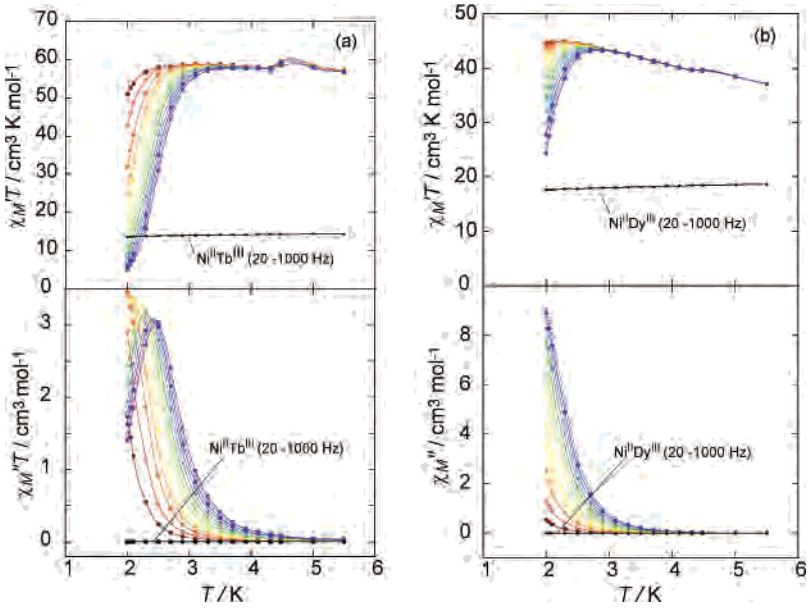

Figure 6. Plots of the in-phase $\chi_M'T$ signal (top row) vs T and out-of-phase χ_M'' (bottom row) signal vs T in ac magnetic susceptibility, where the frequencies for $Cu^{II}_2Tb^{III}_2$ and $Cu^{II}_2Dy^{III}_2$ complexes are 20, 50, 100, 150, 200, 300, 400, 500, 600, 700, 800, 900, and 1000 Hz. (a) $Cu^{II}_2Tb^{III}_2$ (top curves) and $Ni^{II}_2Tb^{III}_2NiTb$ (bottom curve). (b) $Cu^{II}_2Dy^{III}_2$ (top curves) and $Ni^{II}_2Dy^{III}_2$ (bottom curve). The plots of the $Ni^{II}_2Tb^{III}_2$ and $Ni^{II}_2Dy^{III}_2$ showed no frequency dependence.

ferromagnetic. As shown in Figure 4, the $\Delta(T)$ values for the complexes with Ce, Pr, Nd, Eu, and Yb (ca. <1 $cm^3 \cdot K \cdot mol^{-1}$) are close to that of $2(\chi_M T)_{Cu} = 0.75$ $cm^3 \cdot K \cdot mol^{-1}$, suggesting negligible or very weak magnetic interaction. Among them, the $\Delta(T)$ value of Ce and Nd complexes decreases from 0.75 $cm^3 \cdot K \cdot mol^{-1}$ in the higher temperature region with the decrease of the temperature, suggesting weak antiferromagnetic interactions at low temperature. On the other hand, as shown in Figure 4b, the $\Delta(T)$ values for the complexes with Gd, Tb, Dy, Ho, Er, and Tm are larger than 0.75 $cm^3 \cdot K \cdot mol^{-1}$ and increase on lowering the temperature, indicating stronger ferromagnetic interactions. This is especially true for the complexes with Gd, Tb, Dy, and Er, for which $\Delta(T)$ reaches particularly high values, suggesting relatively strong interactions. Interestingly, the $Cu^{II}_2Tb^{III}_2$ complex seems to have the larger $\Delta(T)$ value at all temperatures.

Analogous informations on the magnetic interactions between Cu^{II} and Ln^{III} ions can be obtained by applying the same empirical approach to the magnetization values. Let us now define Δ as $\Delta(H) = M_{Cu2Ln2}(H) - M_{Ni2Ln2}(H)$, where M is the magnetization measured on the complex denoted by the subscript. By assuming again negligible $Ln^{III}-Ln^{III}$ and $Cu^{II}-Cu^{II}$ interactions, this parameter Δ may be obtained from the relation $\Delta(H) = M_{Cu2Ln2}(H) - M_{Ni2Ln2}(H) = 2M_{Cu}(H) + 2J_{CuLn}(H)$, where $2M_{Cu}(H)$ is the magnetization for two independent Cu^{II} ions that can be calculated by the Brillouin function while the extra contribution $2J_{CuLn}(H)$ is related to the nature of the overall exchange magnetic interactions between the Cu^{II} and Ln^{III} ions. As the quantity $(\Delta(H) - 2M_{Cu}(H))$ represents the deviation from the limit situation of magnetically independent Cu^{II} and Ln^{III} ions, positive values of $J_{CuLn}(H)$, i.e., $\Delta(H)$ lying above $2M_{Cu}(H)$, indicate ferromagnetic $Cu^{II}-Ln^{III}$ interactions while negative values of $J_{CuLn}(H)$, i.e., $\Delta(H)$ lying below $2M_{Cu}(H)$, indicate antiferromagnetic $Cu^{II}-Ln^{III}$ interactions.

The values of the parameter $\Delta(H)$ are plotted in Figure 5a,b for all compounds and compared with the Brillouin function of two independent Cu^{II} ions. From Figure 5a, we see that the $\Delta(H)$ versus H plots for La, Pr, Eu, and Lu are very close to the theoretical values of $2M_{Cu}(H)$, indicating no detectable magnetic interactions in these complexes,

where La^{III} and Lu^{III} ions are diamagnetic. The plots for Ce, Nd, Sm, and Yb lie a little below $2M_{Cu}(H)$ in the whole range of H, suggesting a weak antiferromagnetic nature of the interaction. Figure 4b shows that the $\Delta(H)$ versus H plots for Gd, Tb, Dy, Ho, Er, and Tm lie well above $2M_{Cu}(H)$ in the whole range of H, thus confirming the ferromagnetic nature of the interaction between Cu^{II} and Ln^{III} ions. The $\Delta(H)$ values for Gd, Tb, Dy, and Er are not only larger than the $2M_{Cu}(H)$ value but also show a steep initial increase up to a maximum occurring between 0.2 and 0.7 T, and then remain almost constant.

Regarding the nature of the magnetic interaction between Cu^{II} and Ln^{III} ions in these complexes, the results from the field dependent magnetization measurements are consistent not only with the results from the temperature-dependent magnetic susceptibility measurements, but also with the results of dinuclear $[Cu^{II}Ln^{III}]$ complexes by Costes et al.,[14] 2D ladder-type $[Ln^{III}_2Cu^{II}_3]$ complexes by Kahn et al.,[15] and trinuclear complexes $[Cu^{II}_2Ln^{III}(L)_2(NO_3)_2]$ with H_2L = 2,6-di(acetoacetyl)pyridine by Okawa et al.[16]

Alternating Field Magnetic Properties of $Cu^{II}_2Ln^{III}_2$ Complexes with Ln = Gd, Tb, Dy, Ho, Er, and Tm. The six $Cu^{II}_2Ln^{III}_2$ complexes exhibiting ferromagnetic interactions have been further examined by ac magnetic susceptibility measurements, since one of the characteristics of an SMM is the observation of an out-of-phase (χ_M'') ac susceptibility signal. The temperature dependent ac magnetic measurements were carried out in a 3.0 G field oscillating at the indicated frequencies (1−1000 Hz) and with a zero dc field, down to the lowest temperature of 1.8 K. Complexes with Tb and Dy exhibit a frequency dependence of the χ_M' and χ_M'' signals, while other complexes with Gd, Ho, Er, and Tm show no frequency dependence under the experimental conditions. Figure 6a shows the results of the ac magnetic susceptibility measurements for $Cu^{II}_2Tb^{III}_2$ and $Ni^{II}_2Tb^{III}_2$ complexes, as plots of $\chi_M'T$ and χ_M''. Figure 6b shows the results of the ac magnetic susceptibility measurements for $Cu^{II}_2Dy^{III}_2$ and $Ni^{II}_2Dy^{III}_2$. The out-of-phase component χ_M'' of both $Cu^{II}_2Tb^{III}_2$ and $Cu^{II}_2Dy^{III}_2$ complexes shows frequency dependence, but a maximum in χ_M'' is only observed for $Cu^{II}_2Tb^{III}_2$. We have examined whether the slow relaxation of the magnetization really arises from the ferromagnetic coupling in $Cu^{II}_2Tb^{III}_2$ and $Cu^{II}_2Dy^{III}_2$ complexes or if it is just intrinsic to the Tb^{III} and Dy^{III} centers by studying the analogous complexes $Ni^{II}_2Tb^{III}_2$ and $Ni^{II}_2Dy^{III}_2$ with Ni^{II} in place of Cu^{II}. As can be seen in Figure 6a,b, $Ni^{II}_2Tb^{III}_2$ and $Ni^{II}_2Dy^{III}_2$ complexes show no frequency-dependent signals in the same temperature range, demonstrating that the present SMM behavior is not due to the sole Tb^{III} or Dy^{III} centers. These results are consistent with those of dinuclear $Cu^{II}-Tb^{III}$ complex studied by Costes et al.[7a]

Figure 7 shows the results of the ac magnetic susceptibility measurements of the complexes with Ho, Er, and Tm as the plots of $\chi_M'T$ versus T and those of χ_M'' versus T. These complexes showed no frequency dependent signals of $\chi_M'T$ and χ_M'', indicating that this complex is not an SMM.

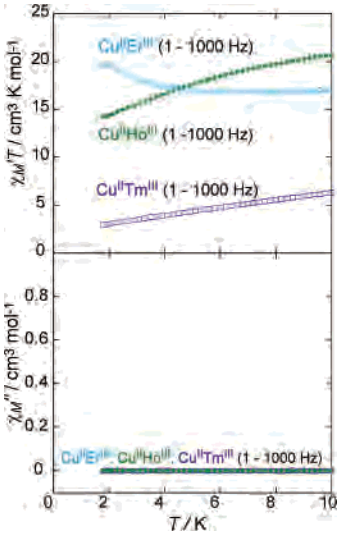

Figure 7. Plots of $\chi_M'T$ and χ_M'' signals for $Cu^{II}_2Ln^{III}_2$ complexes (Ln = Ho, Er, and Tm), showing no frequency dependence, where the frequencies are varied from 1 to 1000 Hz.

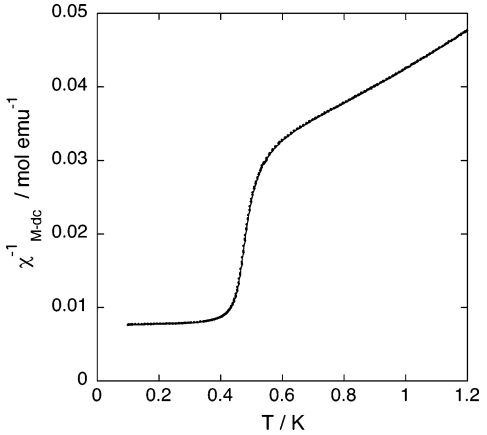

Figure 8. Inverse of the magnetic susceptibility of $Cu^{II}_2Tb^{III}_2$ complex as a function of temperature. The measuring field was 5 Oe, and the sample was cooled from 1.2 K with a cooling rate of 0.15 K/h.

Very Low Temperature Measurements on $Cu^{II}_2Tb^{III}_2$ Complex. Because of the promising dynamic response observed above 1.8 K for the $[Cu^{II}LTb^{III}(hfac)_2]_2$ complex, an additional study at the very low temperature region has been made for this complex, with some surprising results. The inverse of the dc magnetic susceptibility χ^{-1}_{M-dc} is plotted as a function of temperature in Figure 8. A small external magnetic field of 5 Oe was applied at 1.2 K, and the sample was field-cooled (FC) to 0.1 K with a cooling rate of 0.15 K/h.

The weak antiferromagnetic interaction between clusters previously evidenced (see Figure 4b) by a decreasing $\chi_M T$ below 10 K is seen to persist down to approximately 0.5 K in this plot; i.e., the data are more or less linear from 1.2 to 0.6 K, and an extrapolation of this trend to zero intercepts the negative temperature axis. However, below 0.5 K, an abrupt crossover to predominantly ferromagnetic interactions

(14) Costes, J.-P.; Dahan, F.; Dupuis, A.; Laurent, J.-P. *Chem. Eur. J.* **1998**, *4*, 1616−1620.
(15) Kahn, M. L.; Mathoniere, C.; Kahn, O. *Inorg. Chem.* **1999**, *38*, 3692−3697.
(16) Shiga, T.; Ohba, M.; Okawa, H. *Inorg. Chem.* **2004**, *43*, 4435−4446.

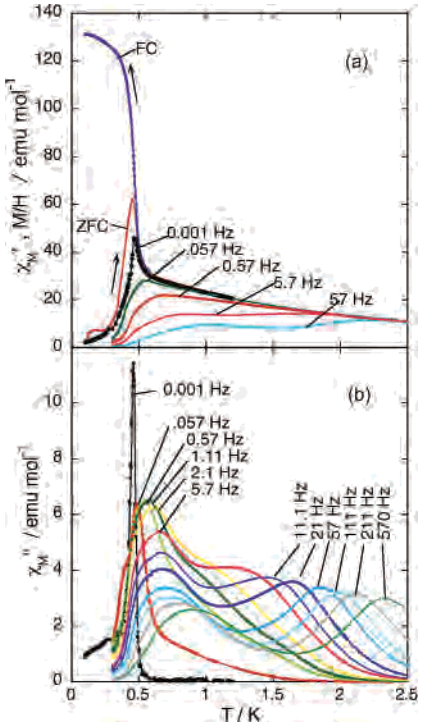

Figure 9. (a) In-phase ac susceptibility χ_M' shown for a few representative frequencies and the zero field cooled (ZFC) and field cooled (FC) dc susceptibility χ_{M-dc} plotted against temperature for $[Cu^{II}LTb^{III}(hfac)_2]_2$. (b) The out-of-phase ac susceptibility χ_M'' shows two distinct peaks for frequencies greater than 5 Hz, but only one peak is observed at low frequency, which becomes very sharp at 0.001 Hz.

takes place. This is seen in Figure 9a, where the same data (blue points) are plotted as χ_{M-dc} versus T.

Below 0.5 K a dramatic increase in the FC susceptibility occurs, which begins to flatten out below 0.4 K. The magnitude of the dc susceptibility at 0.1 K is reasonably close to the saturation value that would occur at a ferromagnetic phase transition. To be specific, when the susceptibility is converted to the units of emu·cm^{-3}, the maximum is within a factor of 2 of $1/N$ where N is the demagnetization factor which we estimate as $4\pi/3$ for this powder sample. Furthermore, relaxation times are very long at low temperature, and as result, the maximum is sensitive to cooling rate: a slower rate results in a higher final maximum. (Note that no corrections have been made to the data for demagnetization effects.) For the acquisition of the zero field cooled (ZFC) dc magnetic susceptibility χ_{M-dc} shown in Figure 9a (red data points), the sample was first cooled from 1.2 K to below 0.1 K in zero field (<0.05 Oe), then a 5 Oe field was applied, and the sample was measured while warming up slowly at the warming rate of 0.15 K/h. A sharp peak is observed at 0.45 K for this warming up rate. The position of this peak is also sensitive to the warming rate, with a slower warming rate resulting in a higher peak occurring at a lower temperature.

Also shown in Figure 9a is the in-phase ac magnetic susceptibility χ_M' for a few representative frequencies. The ac susceptibility measurements were made in a field of 1.4 Oe rms. For frequencies higher than 5 Hz, two peaks can be discerned in the χ_M' susceptibility. For lower frequencies,

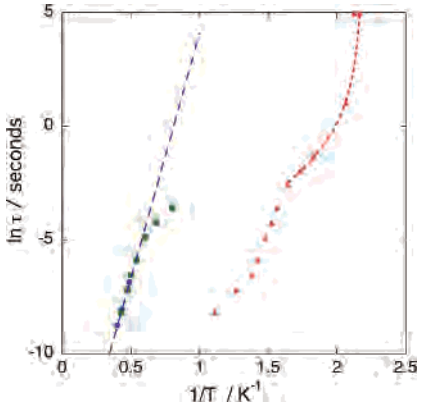

Figure 10. Plot of $\ln(\tau)$ vs $1/T$. The temperature corresponding to a characteristic relaxation time τ was determined by the position of the out-of-phase ac susceptibility χ_M'' peaks in Figure 9b. The high frequency and high temperature (>2 K) data points (blue circles) have been fit to a straight line (dashed blue line). The low frequency and low temperature data points are taken from the peaks in χ_M'' below 1 K. The dashed red line is a fit to the lowest frequency data points with $\tau = \tau_0(T/T_c - 1)^{-z\nu}$ which describes critical slowing down near a phase transition.

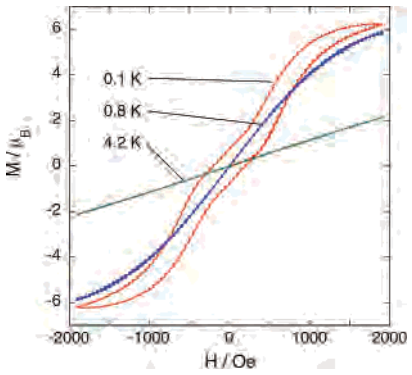

Figure 11. Magnetization as a function of the applied magnetic field at three different temperatures. Notice the opening of the cycle at 0.1 K with a minor loop.

only one peak below 1 K in the susceptibility is observed. Our lowest frequency measurement at 0.001 Hz (corresponding to a period of 16.7 min) displays a sharp cusp at approximately 0.47 K. Note that the 0.001 Hz data points fall on top of the ZFC and FC data above this temperature. During low frequency data acquisition, special care was taken to very slowly warm and cool the sample, so that the curves were reversible. In particular, for the 0.001 Hz curve the temperature was stepped at 0.05 K, with a wait period of 2 h per point.

The out-of-phase ac magnetic susceptibility χ_M'' versus temperature is shown in Figure 9b for various frequencies between 570 and 0.001 Hz. As with the in-phase susceptibility, two distinct peaks for frequencies greater than 5 Hz can also be seen. The high temperature peaks (above 2 K) have been previously reported[4] and correspond to superparamagnetic SMM behavior. At this temperature, the relaxation of the giant spins comes from thermal activation over an energy barrier whose source is the anisotropy of the clusters. On the other hand, only one peak is observed for frequencies below 2 Hz, which becomes increasingly sharp as the frequency decreases. At 0.001 Hz the peak in the out-of-phase ac susceptibility is extremely sharp, and is more like

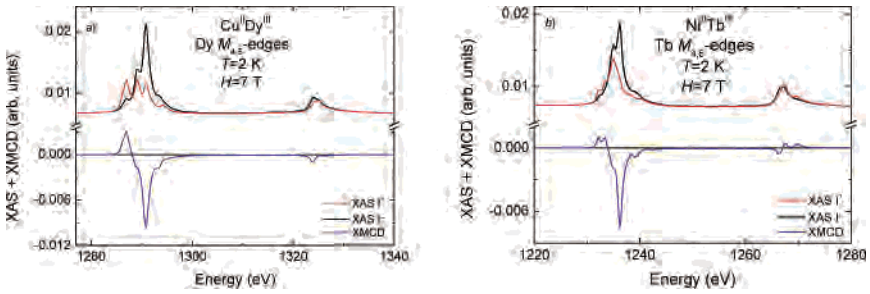

Figure 12. XAS and XMCD spectra of (a) $Cu^{II}_2Dy^{III}_2$ at the Dy $M_{4,5}$-edges and (b) $Ni^{II}_2Tb^{III}_2$ at the Tb $M_{4,5}$-edges measured at 2 K and 7 T. I^+ and I^- denote, respectively, that the helicity of the incoming circular polarized light was parallel or antiparallel to the direction of the magnetic field.

an onset. The cause of the low frequency−low temperature peaks is puzzling.

Among the reasons for the presence of two peaks in the curve of χ''_M, there are two possibilities mentioned, i.e., the presence of two cluster species and the setting-up of a phase transition probably to a ferromagnetic ordered state. For instance, the presence of two peaks has been attributed to the presence of two cluster species for some Mn_{12} complexes[17a] and $Co(carbene)_4$ complexes[17b] and to long-range ordering in $Fe(III)_4$ complexes.[17c]

The frequency dependence of the low temperature peak does not appear to be caused by thermal activation, in contrast to the high temperature peak. This can best be seen in a plot of $\ln(\tau)$ versus $1/T$ as shown in Figure 10. For this plot, the temperature corresponding to a characteristic relaxation time $\tau = 1/\omega$ (i.e., $1/2\pi f$ where f is the frequency) was determined by the position of the out-of-phase ac susceptibility χ_M'' peaks of Figure 9b. The high frequency and high temperature (>50 Hz, >2K) data points (blue circles) can be fitted with a straight line (dashed blue line) which implies that $\tau = \tau_0 + \exp(-E_B/kT)$. From the fit, we find an energy barrier $E_B = 23$ K and $\tau_0 = 2.7 \times 10^{-8}$ s, reasonable values for an SMM. Nevertheless, deviations become apparent for frequencies below 50 Hz. On the other hand, the low frequency and low temperature data points (taken from the set of peaks in χ_M'' that occur below 1 K) clearly cannot be fit with a simple thermal activation law.

Indeed, the very low frequency (<2 Hz) data, with the pronounced sharpening of the peaks, is more indicative of a phase transition, and due to the very large susceptibility, we may speculate that the ordered state is ferromagnetic. This is, however, a rather remarkable transition: it is a "slow-motion" transition, from the superparamagnetic state to the ferromagnetic state, reminiscent of cluster glass transitions, but sharper and more clearly defined. With this in mind, we have fit the lowest frequency data points (f < 2 Hz) with the equation $\tau = \tau_0(T/T_c - 1)^{-z\nu}$ (red dashed line in Figure 10). This equation is used to describe the dynamic behavior of critical slowing down near a phase transition. The fit to the equation gives the critical exponents $z\nu = 2$ and an anomalously large $\tau_0 = 0.01$ s with a $T_c = 0.43$ K.

The magnetization versus applied field was also measured at low temperature, and Figure 11 shows the results for 4.2, 0.8, and 0.1 K. The maximum field of 2000 Oe for this magnetometer was not enough to saturate the sample.

As can be seen in Figure 11, rather complicated minor hysteresis loops open up below 0.4 K. These are intriguing results, and further measurements are planned when large enough single crystals of $[Cu^{II}LTb^{III}(hfac)_2]_2$ will become available.

Table 1. Experimental (from XMCD) and Theoretical (Hund's Rules) Values of the Magnetic Moments

molecule	ion	m_L [μ_B/at.]	m_S [μ_B/at.]	m_{tot} [μ_B/at.]	m_{tot}(Hund) [μ_B/at.]	$\langle L_z\rangle/\langle S_z\rangle$	$\langle L_z\rangle/\langle S_z\rangle$ (Hund)
$Cu^{II}_2Tb^{III}_2$	Tb^{III}	1.9(2)	3.9(3)	5.8(2)	9.0	1.0(2)	1.0
$Cu^{II}_2Tb^{III}_2$	Cu^{II}	0.10(2)	0.56(3)	0.66(3)	3.0	0.35(5)	4.0
$Ni^{II}_2Tb^{III}_2$	Tb^{III}	1.9(2)	3.2(3)	5.1(2)	9.0	1.2(2)	1.0
$Cu^{II}_2Dy^{III}_2$	Dy^{III}	2.5(2)	3.2(3)	5.7(2)	10.0	1.6(2)	2.0
$Cu^{II}_2Dy^{III}_2$	Cu^{II}	0.09(2)	1.04(5)	1.13(5)	3.0	0.17(5)	4.0

XMCD Measurements on the $Cu^{II}_2Tb^{III}_2$, $Cu^{II}_2Dy^{III}_2$, and $Ni^{II}_2Tb^{III}_2$ Complexes. In order to shed some light on the magnetic coupling between the different ions in these molecules, we have performed X-ray absorption spectroscopy (XAS) and X-ray magnetic circular dichroism (XMCD) measurements at the rare-earth $M_{4,5}$-edges (3d−4f transitions), the transition metal $L_{2,3}$-edges (2p−3d transitions), and O and N K-edges (1s−2p transitions), on the three complexes $Cu^{II}_2Tb^{III}_2$, $Cu^{II}_2Dy^{III}_2$, and $Ni^{II}_2Tb^{III}_2$. These techniques allow us to obtain information about the structural and magnetic properties of the molecules with chemical element and valence sensitivity.

Figure 12 shows typical XAS and XMCD spectra measured on $Ni^{II}_2Tb^{III}_2$ and $Cu^{II}_2Dy^{III}_2$ at the $M_{4,5}$-edges of Tb and Dy, respectively, and at a temperature $T = 2$ K in a magnetic field $H = 7$ T. The XAS and XMCD spectra of Tb in $Cu^{II}_2Tb^{III}_2$ are identical in shape to those of Tb in $Ni^{II}_2Tb^{III}_2$ and are not shown. The shape of the Tb and Dy XAS and XMCD spectra shows the multiplet structure that is typical for the trivalent configuration of these ions, with 8 and 9 electrons in the 4f shell, respectively.

A quantitative evaluation of the magnetic moment carried by the Tb and Dy ions in the three molecules can be performed by applying the magneto-optical sum rules[18] to the measured XAS and XMCD spectra. These sum rules allow one to determine independently the orbital ($m_L = \langle L_z\rangle$)

(17) (a) Aubin, S. M. J.; Sun, Z.; Eppley, H. J.; Rumberger, E. M.; Guzei, I. A.; Folting, K.; Gantzel, P. K.; Rheingold, A. L.; Christou, G.; Hendrickson, D. N. *Inorg. Chem.* **2001**, *40*, 2127−2146. (b) Karasawa, S.; Zhou, G.; Morikawa, H.; Koga, N. *J. Am. Chem. Soc.* **2003**, *125*, 13676−13677. (c) Barra, A. L.; Caneschi, A.; Cornia, A.; Fabrizi-Biani, F.; Gatteschi, D.; Sangregorio, C.; Sessoli, R.; Sorace, L. *J. Am. Chem. Soc.* **1999**, *121*, 5302−5310.

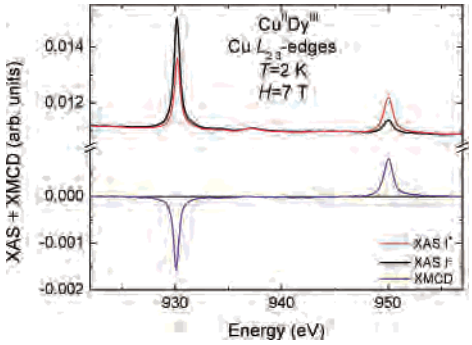

Figure 13. XAS and XMCD spectra of $Cu^{II}_2Dy^{III}_2$ at the Cu $L_{2,3}$-edges measured at 2 K and 7 T. I^+ and I^- denote, respectively, that the helicity of the incoming circular polarized light was parallel or antiparallel to the direction of the magnetic field.

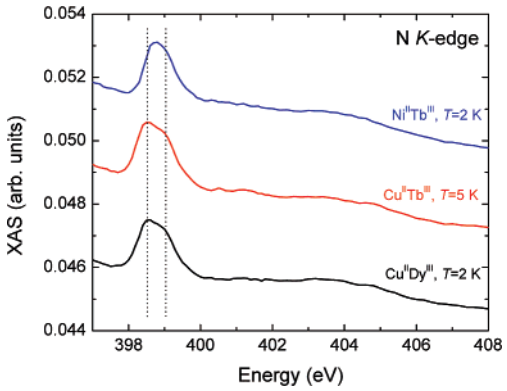

Figure 14. XAS spectra of $Cu^{II}_2Dy^{III}_2$, $Cu^{II}_2Tb^{III}_2$, and $Ni^{II}_2Tb^{III}_2$ at the N K-edge. The three spectra have been shifted with respect to one another for clarity. The dotted lines indicate the positions of the two partially resolved peaks of $Cu^{II}_2Dy^{III}_2$ and $Cu^{II}_2Tb^{III}_2$.

and spin ($m_S = 2\langle S_z\rangle$) magnetic moments contributing to the total magnetic moment $m_{tot} = m_L + m_S$. The values of m_L, m_S, and m_{tot} obtained for the three molecules at 2 K and 7 T are listed in Table 1. In all three cases, the total magnetic moment is considerably reduced (by a factor close to 2) with respect to the values expected for the free ions Tb and Dy according to Hund's rules. A possible simple explanation for this behavior would be that a field of 7 T might not be sufficient to saturate the paramagnetic moments of the rare earths in the molecules. However, the magnetic moments measured at 5 K and 7 T coincide within the error bars to those obtained at 2 K, thus suggesting that the paramagnetic moments are indeed (almost) completely aligned by the field of 7 T. Most likely, the reduction observed in the magnetic moments arises from the effect of the crystal field, as already found previously in Dy@C_{82} and Dy@C_{88} endohedral fullerenes.[19] The crystal field interaction, whose energy is typically on the order of ~10−100 meV in 4f electron systems, has no directly visible effect in the shape of the XAS and XMCD signals at the $M_{4,5}$ edges of rare earths, because it is negligible as compared to the large intrinsic energy widths (~1 eV) of these 3d−4f transitions. However, the crystal field interaction usually has a sizable effect on the ratio $\langle L_z\rangle/\langle S_z\rangle$ and/or on the absolute value of the total magnetic moment (because of the strong spin−orbit coupling). In the present case, this ratio remains very close to its free ion value (see Table 1), and only the total magnetic moment is considerably reduced. It is also worthwhile to mention that the Tb magnetic moment appears to be smaller in $Ni^{II}_2Tb^{III}_2$ than in $Cu^{II}_2Tb^{III}_2$.

Figure 13 shows the Cu $L_{2,3}$-edge XAS and XMCD measured at 2 K and 7 T on $Cu^{II}_2Dy^{III}_2$. Again, the spectra measured on $Cu^{II}_2Tb^{III}_2$ are identical, within the error, to those of $Cu^{II}_2Dy^{III}_2$. The XAS spectrum consists of two sharp peaks at E = 930 eV and E = 950 eV, corresponding to the L_3 and L_2 thresholds, respectively, and two weak peaks at ~934 and 937 eV (which will not be further discussed here). The XMCD is strong and negative at the L_3 threshold, while it is positive at the L_2. Also, in the case of the $L_{2,3}$-edges of Cu, the magneto-optical sum rules can be applied to determine spin and orbital magnetic moments carried by the Cu^{II} ions ($3d^9$ configuration) in these molecules, which are shown in Table 1. For both molecules, the orbital magnetic moment m_L is almost completely quenched by the crystal field, as is usual for the transition metals. The total magnetic moment is aligned parallel to that of the rare earth, thus confirming the ferromagnetic coupling already inferred from the dc susceptibility measurements. However, the total Cu moment of $Cu^{II}_2Dy^{III}_2$ is about a factor of 2 larger than that of $Cu^{II}_2Tb^{III}_2$.

Figure 14 shows the N K-edge XAS spectra of $Cu^{II}_2Tb^{III}_2$, $Ni^{II}_2Tb^{III}_2$, and $Cu^{II}_2Dy^{III}_2$. For all three molecules most of the absorption is concentrated in the energy interval between 398 and 400 eV, which can be related to the hybridization between the N 2p and the Cu or Ni 3d electrons. In the case of the $Cu^{II}_2Tb^{III}_2$ and $Cu^{II}_2Dy^{III}_2$ complexes, two partially resolved peaks are observable (at 398.5 and 399 eV, dotted lines in Figure 14), while only one is visible at 398.8 eV for the $Ni^{II}_2Tb^{III}_2$ complex. No XMCD signal was observed on any of the molecules, which is likely to arise from the fact that N is not directly involved in the bonds bridging Cu/Ni with Tb/Dy. However, the high level of noise in these measurements does not allow us to rule out the presence of a magnetic polarization of all or some of the N atoms.

Figure 15a shows the O K-edge XAS spectra of $Cu^{II}_2Tb^{III}_2$, $Ni^{II}_2Tb^{III}_2$, and $Cu^{II}_2Dy^{III}_2$. The general appearance of the XAS spectra is similar for all molecules, with two partially resolved pre-peaks at energies of 530.6 and 531.8 eV, which can be attributed to the hybridization between the O 2p and the Cu/Ni 3d electrons, followed by a broad bump centered at about 539 eV. The different shape and intensity ratio of the pre-peaks might reveal differences in the Cu−O hybridization between $Cu^{II}_2Tb^{III}_2$ and $Cu^{II}_2Dy^{III}_2$, which might in turn explain the differences observed in the value of the Cu^{II} ion total magnetic moments. In both cases, weak XMCD signals (see Figure 15b) are observed at an energy corresponding approximately to that of the first pre-peak, indicating the presence of small magnetic moments

(18) (a) Carra, P.; Thole, B. T.; Altarelli, M.; Wang, X. *Phys. Rev. Lett.* **1993**, *70*, 694. (b) Thole, B. T.; Carra, P.; Sette, F.; van der Laan, G. *Phys. Rev. Lett.* **1992**, *68*, 1943.

(19) (a) De Nadaï, C.; Mirone, A.; Dhesi, S. S.; Bencok, P.; Brookes, N. B.; Marenne, I.; Rudolf, P.; Tagmatarchis, N.; Shinohara, H.; Dennis, T. J. S. *Phys. Rev. B* **2004**, *69*, 184421. (b) Bondino, F.; Cepek, C.; Tagmatarchis, N.; Prato, M.; Shinohara, H.; Goldoni, A. *J. Phys. Chem. B* **2006**, *110*, 7289.

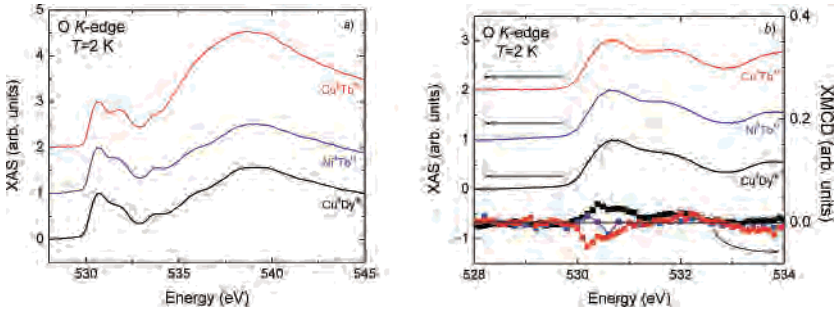

Figure 15. (a) XAS spectra of $Cu^{II}_2Dy^{III}_2$, $Cu^{II}_2Tb^{III}_2$, and $Ni^{II}_2Tb^{III}_2$ at the O K-edge. The three spectra have been shifted with respect to one another for clarity. (b) Zoom around the pre-peaks region, showing both XAS and XMCD signals for the three molecules (solid lines indicate helicity antiparallel to magnetic field, and squares with line indicate XMCD).

on those of the O atoms that are directly involved in the bonds bridging the Cu^{II} with the rare earth atoms (see Scheme 1). It is remarkable to observe that the sign of this XMCD signal is opposite in $Cu^{II}_2Tb^{III}_2$ and $Cu^{II}_2Dy^{III}_2$, indicating that the O 2p magnetic moments are oriented in opposite directions in the two molecules. There is no XMCD signal detectable at the O *K*-edge of $Ni^{II}_2Tb^{III}_2$, which can be explained by the fact that there is no magnetic coupling between neighboring Tb^{III} and Ni^{II} ions in this molecule, owing to the fact that Ni^{II} is in its low spin state and is therefore diamagnetic. However, the XMCD signals at the O *K*-edge are extremely weak and the signal-to-noise ratio particularly unfavorable for these measurements on powdered samples. In the future, high quality measurements on single crystals should confirm the presence of these XMCD signals.

Concluding Remarks. A whole series of tetranuclear $Cu^{II}_2Ln^{III}_2$ complexes $[Cu^{II}LLn^{III}(hfac)_2]_2$ involving all lanthanide(III) ions except the radioactive Pm^{III} has been prepared. Unfortunately, it is still difficult to give a clear answer to the question raised at the beginning of this paper, namely what makes some molecules SMMs and others not. Comparison of the magnetic properties of the $Cu^{II}_2Ln^{III}_2$ complexes with those of the corresponding $Ni^{II}_2Ln^{III}_2$ complexes revealed that the magnetic interaction between Cu^{II} and Ln^{III} ions with Ln = Ce, Nd, Sm, and Yb is very weakly antiferromagnetic, that with Ln = La, Eu, Pr and Lu shows no significant magnetic interaction, and that with Ln = Gd, Tb, Dy, Ho, Er, and Tm is ferromagnetic. Among the six $Cu^{II}_2Ln^{III}_2$ complexes exhibiting ferromagnetic interaction, only two complexes with Tb and Dy showed a frequency dependence of χ_M' and χ_M'', and were therefore expected to be SMMs, while the other complexes with Gd, Ho, Er, and Tm showed no frequency dependence under the same experimental conditions. With the goal of better understanding the evolution of the intramolecular magnetic interactions, X-ray magnetic circular dichroism (XMCD) has also been measured on $Cu^{II}_2Tb^{III}_2$, $Cu^{II}_2Dy^{III}_2$, and $Ni^{II}_2Tb^{III}_2$ complexes, both at the *L*- and *M*-edges of the metal ions and at the *K*-edge of the N and O atoms. We observe that the moment on the 4f ions is lower than what is predicted by Hund's rule, that the orbital moment on the copper ions is almost completely quenched, and that the moments on the 3d and 4f ions are parallel, which confirms the ferromagnetic coupling deduced from SQUID observations. While no magnetic polarization could be measured on the N atoms, some amount has been detected on the oxygen. We believe that this is very important, since the magnetic intramolecular couplings within these SMM usually pass through light elements such as O. It has unfortunately not been possible to perform these measurements below 2 K. One should probably observe a more intense signal below the blocking temperature. Last, the $Cu^{II}_2Tb^{III}_2$ complex exhibiting SMM behavior has received a closer examination of its low temperature magnetic properties down to 0.1 K. These particular measurements have revealed an unexpected behavior at low temperature which could probably be ascribed to the very slow setting-up of a 3D order below 0.6 K. More experiments will be performed on single crystals and at lower temperatures as soon as possible. Regarding the magnetic polarization of the N and O, in addition to the gathering of more experimental data with polarized neutrons or XMCD, it becomes more and more important that some theoretical calculations and modeling start being developed.

Experimental Section

Materials. All chemicals and solvents used for the synthesis were reagent grade and were obtained from Tokyo Kasei Co. Ltd and Wako Co. Ltd. and used without further purification. Component complexes, $K[Cu^{II}L]$, $K[Ni^{II}L]\cdot 2H_2O$, and $Ln(hfac)_3(H_2O)_2$, were prepared according to the method reported previously,[13] where the ligand H_3L is 1-(2-hydroxybenzamido)-2-(2-hydroxy-3-methoxybenzylideneamino)ethane and Hhfac is hexafluoroacetylacetone.

$Cu^{II}_2Ln^{III}_2$ Complexes, $[Cu^{II}LLn^{III}(hfac)_2]_2$. The syntheses of the tetranuclear $Cu^{II}_2Ln^{III}_2$ and $Ni^{II}_2Ln^{III}_2$ complexes with Ln^{III} = Eu^{III}, Gd^{III}, Tb^{III}, and Dy^{III} were reported previously. The other tetranuclear $Cu^{II}_2Ln^{III}_2$ and $Ni^{II}_2Ln^{III}_2$ complexes with Ln = La, Ce, Pr, Tm, Yb, and Lu were newly prepared in this study according to the similar synthetic method of those for $Cu^{II}_2Ln^{III}_2$ and Ni^{II}_2-Ln^{III}_2 complexes with Ln = Eu, Gd, Tb, and Dy.[12] The synthesis of $[Cu^{II}LGd^{III}(hfac)_2]_2$ is exemplified. A methanolic solution (20 mL) of $K[Cu^{II}L]$ (0.104 g, 0.25 mmol) was gently poured into a methanolic solution (20 mL) of $Gd(hfac)_3(H_2O)_2$ (0.203 g, 0.25 mmol) at ambient temperature. The resulting solution was allowed to stand for several days. The solution became almost colorless, and the crystals that formed were collected by filtration and dried in air. The crystals were sparingly soluble even in *N*,*N*′-dimethylformamide (DMF), and recrystallization was not performed. Dark reddish purple crystals were obtained. Yield: 0.208 g (88%). The elemental analytical data of C, H, and N for 14 complexes agree well with the calculated values of $[Cu^{II}LLn^{III}(hfac)_2]_2$ which are deposited as Supporting Information.

$Ni^{II}_2Ln^{III}_2$ Complexes, $[Ni^{II}LLn^{III}(hfac)_2]_2$. This complex was prepared by the same method as for $[Cu^{II}LLn^{III}(hfac)_2]_2$, using $K[Ni^{II}L]\cdot 2H_2O$ instead of $K[Cu^{II}L]$. Orange microcrystals were obtained. Yield: 0.195 g (85%). The elemental analytical data of C, H, and N for 14 complexes agree well with the calculated values of $[Ni^{II}LLn^{III}(hfac)_2]_2$ which are deposited as Supporting Information.

Physical Measurements. Elemental C, H, and N analyses were carried out at the Instrumental Analysis Center of Kumamoto University. Infrared spectra were recorded on a Nicolet Avatar 370 DTGS spectrometer using KBr disks. Temperature-dependent dc magnetic susceptibilities in the temperature range 2−300 K and field-dependent magnetization in an applied magnetic field from 0 to 5 T at 2.0 K were measured with an MPMS-5S SQUID susceptometer (Quantum Design, Inc.) at Kumamoto University. All samples were 3 mm diameter pellets molded from ground crystalline samples. The calibrations were performed with palladium. Corrections for diamagnetism were applied using Pascal's constants. Alternating current magnetic measurements were carried out at University of Wroclaw in a 3.0 G ac field oscillating at indicated frequencies (1−1000 Hz). Low temperature dc magnetization and ac susceptibility measurements were preformed using a SQUID magnetometer equipped with a miniature dilution refrigerator developed at the CRTBT-CNRS in Grenoble. Absolute values of the magnetization can be made by the extraction method down to 70 mK. In order to ensure good thermal contact at low temperature, vacuum grease was mixed with 0.028 g of powder $[Cu^{II}LTb^{III}(hfac)_2]_2$ sample and pressed into a small Cu pouch. The XMCD measurements were performed at the soft X-ray beamline UE46 of Bessy, Berlin, Germany, with an energy resolution $E/\Delta E \sim 8000$ and a rate of circular polarization greater than 90%. The powdered samples were mixed with graphite, in order to ensure good thermal and electrical contact with the Cu sample holder, and inserted into an ultrahigh-vacuum cryomagnet system, allowing us to reach temperatures down to 2 K and magnetic fields up to 7 T. The XAS and XMCD signals were obtained in the total electron yield (TEY) mode, by measuring the drain current of the sample.

Acknowledgment. This work was supported in part by a Grant-in-Aid for Science Research (nos. 16655023 and 16205010) from the Ministry of Education, Science, Sports, and Culture, Japan and by the Polish Ministry of Science and Higher Education No. 1T09A 12430. Synchrotron experiments have been performed at BESSY with financial support from the European Community-Research Infrastructure Action under the FP6 "Structuring the European Research Area" Programme (through the Integrated Infrastructure Initiative "Integrating Activity on Synchroton and Free Electron Laser Science-Contract R II 3-CT-2004-506008"). We would like to thank Bernard Muller and Fabrice Maingot for their much appreciated help with the experimental setup.

Supporting Information Available: Tables of properties of ground states of Ln^{III} ion and elemental analytical data. This material is available free of charge via the Internet at http://pubs.acs.org.

IC062252S